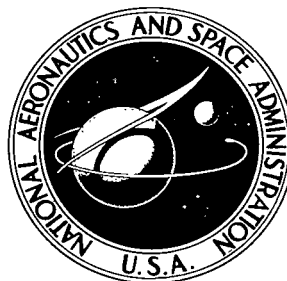


NASA TECHNICAL NOTE

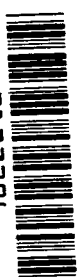


NASA TN D-5366

c.1

LOAN COPY: RETURN
AFWL (WLIL-2)
KIRTLAND AFB, N M

0132296



TECH LIBRARY KAFB, NM

NASA TN D-5366

EFFECTS OF NICKEL ON THE PERFORMANCE OF N ON P SILICON SOLAR CELLS

by Cosmo R. Baraona
Lewis Research Center
Cleveland, Ohio



0132296

EFFECTS OF NICKEL ON THE PERFORMANCE OF
N ON P SILICON SOLAR CELLS

By Cosmo R. Baraona

Lewis Research Center
Cleveland, Ohio

NATIONAL AERONAUTICS AND SPACE ADMINISTRATION

For sale by the Clearinghouse for Federal Scientific and Technical Information
Springfield, Virginia 22151 - CFSTI price \$3.00

ABSTRACT

Nickel was added to 10-ohm-cm boron-doped silicon by a floating-zone technique. The calculated nickel concentrations were about 10^{14} atoms/cm³. Solar cells were made by a standard process. Diffusion length, spectral response, and current-voltage characteristics were measured before and after bombardments by 1-MeV electrons with fluences ranging from 1×10^{14} to 1.5×10^{16} per cm². Nickel decreases the initial solar cell performance and does not improve the radiation resistance of the cell. The decreased performance is probably caused by nickel precipitation.

EFFECTS OF NICKEL ON THE PERFORMANCE OF N ON P SILICON SOLAR CELLS

by Cosmo R. Baraona

Lewis Research Center

SUMMARY

Nickel (Ni) was added to silicon (Si) by a floating-zone technique called the starting-charge-only method. This technique makes it possible to selectively dope with Ni parts of a boron-containing Si crystal. Two crystals with two different Ni concentrations were grown. Each crystal had a section that did not contain Ni and served as an experimental control. Wafers cut from each crystal were fabricated into solar cells by a standard process. Included in the process were a low-temperature, short-time junction diffusion and a vacuum evaporation of contacts. The minority carrier diffusion lengths (related to lifetime) were measured by an X-ray method. Spectral responses were obtained with a filter-wheel solar simulator. Current-voltage curves were measured under tungsten illumination. The cells were bombarded with 1-MeV electrons, and their performance was measured.

This investigation of the effects of nickel in 10-ohm-centimeter boron-doped silicon solar cells showed that it is possible to add nickel to silicon with concentrations in the range of 10^{14} atoms per cubic centimeter. These low concentrations of nickel in 10-ohm-centimeter boron-doped, N on P silicon solar cells do not improve the radiation resistance of the cells. Nickel also lowers the initial minority carrier diffusion length and impairs the spectral response of N on P silicon solar cells. The initial loss of diffusion length and spectral response is not recovered during the course of bombardment by 1-MeV electrons. The degrading action of Ni probably results from Ni precipitation.

INTRODUCTION

Silicon solar cells convert sunlight into electricity and are the most common source of power for unmanned space satellites. Space satellites and their solar power supplies are bombarded by energetic electrons and protons from the Van Allen radiation belts

surrounding the Earth. Radiation creates defects (recombination centers) in the silicon crystal lattice that decrease the charge carrier lifetime and the related carrier diffusion length. Decreased diffusion length lowers cell current and voltage output.

This undesirable loss of output can be reduced by three methods. First, the cells can be shielded with cover glasses (ref. 1). Second, the less radiation sensitive blue response (i. e. , power output due to blue light, ref. 2) can be increased by optimizing junction depth. Both of these areas have been investigated. A third method involving the use of impurities has not been studied extensively.

Impurities intentionally added to the bulk silicon may move to and neutralize the recombination centers caused by the radiation. To be useful in reducing radiation damage, an impurity should not degrade cell performance and must be mobile within the crystal lattice. The addition of lithium (ref. 3) has shown potential for improving solar cell radiation stability.

Nickel is an impurity that has exhibited interesting properties in silicon. Silverman and Singleton (ref. 4) observed that the low lifetime of N on P silicon diodes could be significantly improved by plating nickel onto the diodes and subsequently heating them above the Ni-Si eutectic temperature. The minority carrier lifetimes in these devices had been degraded during junction diffusion and were less than 1 microsecond. After Ni plating and reheating, the lifetime increased to about 10 microseconds. In 1966, Abdullayev et al. (ref. 5) reported similar results.

In view of these previous results, the purpose of this work was to investigate the effects of Ni doping on the radiation resistance of silicon solar cells. An unsuccessful attempt was made to use the plating and heat-treating techniques of Silverman and Singleton on shallow-junction ($0.5\ \mu\text{m}$) solar cells. Nickel was added to silicon by the floating-zone technique (ref. 6). The resulting Ni-doped Si was fabricated into solar cells. About 30 control cells that did not contain Ni and 56 cells that contained Ni were made and evaluated. The cells were bombarded with 1-MeV electrons to fluences (time-integrated flux) of about 10^{16} per square centimeter. Cell properties that were measured before and after various levels of bombardment included diffusion length, spectral response, and current-voltage characteristics.

PROCEDURE

Material Preparation

Doping theory. - An understanding of the effective distribution coefficient K is essential for planning doping experiments of Si single crystals. The effective distribution coefficient is defined as the solute concentration in the solid C_S divided by the solute concentration in the main body of the liquid C_L :

$$K = \frac{C_S}{C_L} \quad (1)$$

If K is much less than 1, the impurity tends to remain in the liquid when a floating liquid zone passes through a solid Si rod. On the other hand, if K is approximately equal to 1, the impurity concentration tends to remain constant when a floating zone passes through a solid Si rod. For Ni in Si, K is approximately 10^{-6} , which indicates that Ni tends to stay in the liquid phase. It is thus very difficult to grow a heavily doped Ni-containing Si single crystal from a melt.

Good solar cell performance occurs when the base region of the cell is in the resistivity range of 10 ohm-centimeters, which corresponds to approximately 10^{15} electrically active impurities per cubic centimeter. Because Ni cannot be doped into Si in this high concentration, boron (B) was used to reduce the resistivity of the Si to the 10-ohm-centimeter level. It was then necessary to obtain a uniform concentration of Ni in the B-doped Si.

The starting-charge-only technique of zone leveling was used to dope the Ni into Si that contained B. In the starting-charge-only method, the Ni is put into the initial molten Si zone only. This zone is then swept along the rest of the ingot. Because of its low distribution coefficient, the Ni will then be uniformly distributed along the entire length of the grown crystal. Because of the high distribution coefficient of boron ($K = 0.8$), only the boron concentration in the first zone to melt and the last zone to freeze was changed from the 10-ohm-centimeter initial value. This change in boron concentration occurs because, once the liquid zone saturates with B, it rejects as much B into the solid as it accepts. Hence, the first region to be zone refined is depleted of B and has a resistivity higher than 10 ohm-centimeters. The last zone to freeze has an excess of B, resulting in a resistivity lower than 10 ohm-centimeters.

Growth technique. - Commercially produced, 10-ohm-centimeter boron-doped float-zone single crystals of silicon were used as starting material. These crystals were about 2 centimeters in diameter by 20 centimeters long and had a (111) orientation. A small hole was sandblasted into the middle of the crystal with 50-micrometer aluminum oxide abrasive. The crystal was then cleaned with the highest purity organic solvents available. Alkaline soap and tap water, trichlorethylene, acetone, isopropyl alcohol, and distilled deionized water were used. The crystal was then etched with a mixture of two parts nitric acid, three parts acetic acid, and one part hydrofluoric acid. The etching was quenched with methyl alcohol, and the crystal was rinsed with distilled water. An accurately weighed charge of 99.999 percent pure Ni powder was then added to the hole. Table I lists the impurities contained in the Ni powder and the method of analysis. The crystal was then carefully mounted in the float-zone apparatus.

TABLE I. - ANALYSIS OF HIGH-PURITY

NICKEL POWDER

Impurity	Maximum limits of impurity, ppm	
	Chemical analysis	Spectrographic analysis
Oxygen	2420	---
Carbon	134	---
Nitrogen	67	---
Silicon	----	10
Iron	----	5
Aluminum	----	<1
Calcium	----	<1
Chromium	----	<1
Copper	----	<1
Silver	----	<1
Magnesium	----	<1

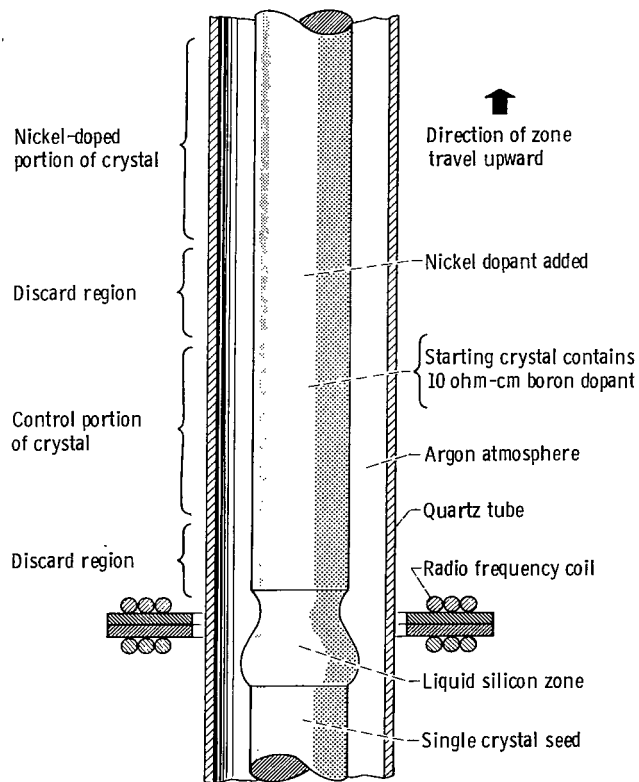


Figure 1. - Zone refining apparatus.

The float-zone refining was done in a clean 35-millimeter-outside diameter quartz tube (see fig. 1). High-purity argon gas was passed through the tube at a rate of 7 liters per minute. The crystal was heated with radiofrequency waves from a coil surrounding the water-cooled quartz tube. The bottom part of the crystal was rotated during the zone pass. The zone traveled upward, and the Ni was uniformly distributed only along the upper half of the crystal. Because K for Ni was small, only one zone pass was used to distribute the Ni (ref. 6). A second zone pass would have removed all the Ni from the crystal.

After the single zone pass, the crystal was cooled to room temperature in the argon atmosphere. It was then taken out of the apparatus and cut into sections. The wafers to be fabricated into solar cells were selected from regions of the crystal where the dopant concentrations in the floating zone had attained constant values. As shown in figure 1, allowance was made for initial B or Ni saturation in the liquid zone and for possible Ni back diffusion into the control portion of the crystal. At least 3 centimeters of crystal between the Ni and control portions (discard regions) were not used. This 3-centimeter safety margin proved to be adequate for two reasons. First, all solar cells made from control regions had a performance typical of 10-ohm-centimeter boron-doped solar cells. Second, all control cells had a performance unlike that of the Ni-containing cells.

Growth results. - Solar cells were made from two ingots, each containing a Ni-doped section. The Ni concentration in the ingots was calculated, since it was too low to be accurately detected by standard analytical techniques. The Ni concentration was calculated from the weight of the Ni charge added to the Si during crystal growth:

$$C_S = \frac{KWN_0}{VA} \quad (2)$$

where C_S is the concentration of Ni in the solid Si, W is the weight of Ni added, N_0 is Avagadro's number, A is the atomic weight of Ni, and V is the 6-cubic centimeter volume of the floating liquid zone.

The first crystal, to which 60 milligrams of Ni powder had been added, had a section containing 1×10^{14} atoms per cubic centimeter calculated concentration of Ni. This crystal also had a boron-doped control section that did not contain Ni. Solar cells made from these sections are labeled 2-Ni and 2-C, respectively. The second crystal, to which 140 milligrams of Ni powder had been added, contained 2.4×10^{14} atoms of Ni per cubic centimeter. From this crystal, cells made from Ni-containing and control portions are labeled 4-Ni and 4-C, respectively. The factor of two differences in the Ni concentration of the two crystals was enough to show a difference in cell performance.

After zone leveling, all sections of both crystals tested P-type with a hot-probe galvanometer technique. The resistivity was measured by a four-probe method. The

TABLE II. - RESISTIVITY RANGE OF USABLE
SECTIONS OF CRYSTALS

Crystal	Resistivity, ohm-cm	
	Initial	Final
2-C (control) and 2-Ni (nickel)	10.6 to 10.8	9.6 to 11.0
4-C (control) and 2-Ni (nickel)	11.3 to 11.7	11.0 to 13.4

results before and after zone leveling are shown in table II. The resistivity variations along the length of the crystal were random. Any changes in resistivity due to Ni doping were below detectable limits.

Solar Cell Fabrication

The selected regions of each crystal were cut into rectangular wafers. These wafers were numbered consecutively by position along the crystal. The wafers were chemically cleaned and etched by a process similar to the one used to clean the crystals before zone refining. The solar cell junctions (phosphorous containing n-type regions) were diffused at 840° C for 20 minutes by using an oxygen carrier gas flow rate of 4.0 liters per minute. The source of phosphorus was phosphorus pentoxide (P_2O_5), which was vaporized in a 280° C zone of the furnace. The resulting N on P junctions were 0.5 micrometer, deep and the wafers had a sheet resistance of 100 ohms per square. This depth was measured by an angle-lapping and staining technique. Gridded front contacts and rectangular back contacts were applied by a silver-cerium evaporation process (ref. 2) which involved a 550° C, 45-minute sintering operation. The contacts were adherent and ohmic. Antireflection coatings were not applied because they would have introduced an unnecessary variable. The finished solar cells were then ready for evaluation.

APPARATUS AND MEASUREMENTS

Irradiation Apparatus

An electron accelerator was used to bombard the cells with 1-MeV electrons. Sixteen cells at a time were held with spring-loaded clips on a wheel that rotated through the electron beam. The time needed to attain a given fluence ϕ was estimated before-

hand from the rate of charge accumulation on a Faraday cup. After the Faraday cup was replaced by the rotating wheel, it was not possible to monitor the accelerator beam current, which did vary slightly. The effect of this variation on the fluence was estimated from the rate of diffusion length, open-circuit voltage, and short-circuit current variation with fluence. The standard deviation in fluence due to this variation was 13 percent. During the bombardment, the cells were air cooled to within 5° C of room temperature. As a rough check on dose level, standard silicon cells with known diffusion-length degradation rates were included in each group of 16. The measured diffusion lengths qualitatively agreed with the calculated fluences.

Diffusion Length Apparatus

The minority carrier diffusion length L_N of the cells is the average range of the excess electrons in the P-type region before recombining. L_N was determined by an X-ray method (unpublished work by John Lamneck of Lewis Research Center). In the X-ray method, cells are irradiated with an X-ray beam of known intensity, and the resultant short-circuit current generated in the cell by the X-rays is measured. This short-circuit current is related to the diffusion length. The relation between the measured short-circuit current and the diffusion length was obtained from standard cells previously measured by the method described by Rosenzweig (ref. 7). The observed standard deviation (reproducibility) of the measurement of the initial diffusion length was ± 3 micrometers. An error analysis indicated that the major source of error can be attributed to the current measurement. The error in the measurement of the initial diffusion length is no greater than 2.5 percent.

Solar Simulator Apparatus

The spectral response of bombarded and unbombarded cells was measured on a filter-wheel solar simulator (ref. 8). The simulator consists of eight narrow-band-pass monochromatic interference filters and a tungsten light source. The currents generated by the cells were measured by a meter with an accuracy of 1/2 percent of full scale. The result was an error in the current generated by the cells at 0.95-micrometer wavelength that was no greater than 5 percent. The cell outputs were calculated as described in reference 8 and were normalized to a cell area of 2 square centimeters.

Other Measurements

Current-voltage apparatus. - The cells were mounted on a temperature-controlled block under a calibrated, regulated tungsten light source. The block temperature was controlled to $25^{\circ} \pm 2^{\circ}$ C. The voltage-current curves of the cells were traced out with a

variable bias supply and an x, y-plotter (ref. 9). With these plots, determinations were made of the open-circuit voltage V_{OC} (within 1 percent), short-circuit current I_{SC} (within 2 percent), maximum power P_M (within 3 percent), and fill factor (defined as $(P_M/I_{SC}V_{OC}) \times 100$). The 2-percent maximum error of the current measurement resulted from the inability to consistently reset the light intensity. The 1-percent maximum error of the voltage primarily resulted from the temperature variation of the cell mounting block. Only the intensity and not the spectral distribution of the light source was calibrated. Because the performance of bombarded solar cells depends on spectral distribution, the data generated by this apparatus can only be used for a relative comparison of cell performance.

Hall mobility. - The base region majority carrier mobility μ_p was measured by the Hall method. Sample currents were between 1 and 10 milliamperes to avoid heating. Hall and resistivity voltages were measured with a vibrating reed electrometer. A magnetic field strength of 9 kilogauss (0.9 T) was used. An error analysis revealed that the mobility measurement has an error no greater than 1 percent.

Junction and contact properties. - A transistor curve tracer was used to determine the series resistance R_S , the diode reverse current at 0.6 volt I_R , and the dimensionless junction parameter A , which appears in the diode equation (ref. 10). These measurements were used to select cells with the best junction and contact properties for bombardment. The average initial values for bombarded cells are an R_S of approximately 0.3 ohm, an I_R of less than 100 microamperes, and an A of approximately 1.8.

RESULTS

Diffusion-Length Data

Table III(a) shows the average minority carrier diffusion length L_N of unbombarded control and Ni cells of the two different Ni concentrations. The diffusion lengths of the 2-Ni cells are about 20 percent lower than those of the 2-C controls. The diffusion lengths of the 4-Ni cells are 33 percent lower than those of their 4-C controls.

The cells that were selected for electron bombardment had good junction and contact properties and representative diffusion lengths. The number of cells of each type that were bombarded, the average diffusion lengths, and the standard deviations of the bombardment groups are shown in table III(b). Note that the diffusion lengths of the samples chosen for the 4-Ni group were higher than those of the average cells.

TABLE III. - INITIAL DIFFUSION LENGTHS

(a) All cells

Cell type	Total number of cells	Average diffusion length, μm	Standard deviation, μm
2-C (control cell)	9	205	3.5
2-Ni (nickel cell)	34	165	16.3
4-C (control cell)	21	186	8.4
4-Ni (nickel cell)	22	125	20.5

(b) Cells selected for bombardment

Cell type	Number of cells selected	Average diffusion length, L , μm	Standard deviation, μm
2-C (control cell)	6	203	3.0
2-Ni (nickel cell)	21	163	12.2
4-C (control cell)	3	187	1.3
4-Ni (nickel cell)	3	136	3.5

Plots of $\log L$ against $\log \phi$ for the 2-Ni, 2-C and the 4-Ni, 4-C groups are shown in figures 2 and 3, respectively. At no point during the bombardment is the average diffusion length of the Ni cells greater than that of the control cells. Additionally, the change in diffusion length per change in fluence for the Ni cells is close to that of the controls. Thus the initial decrease in solar cell diffusion length per change in fluence for

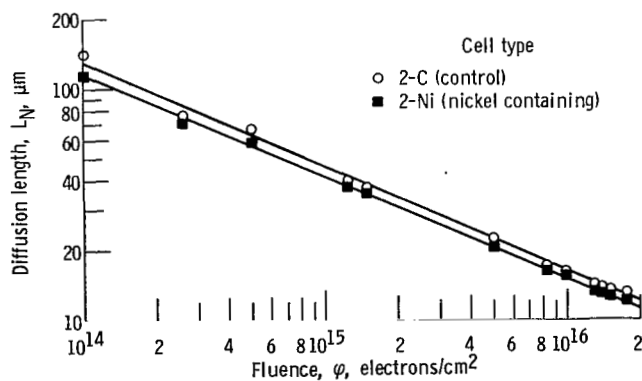


Figure 2. - Diffusion length as function of 1-MeV electron fluence.

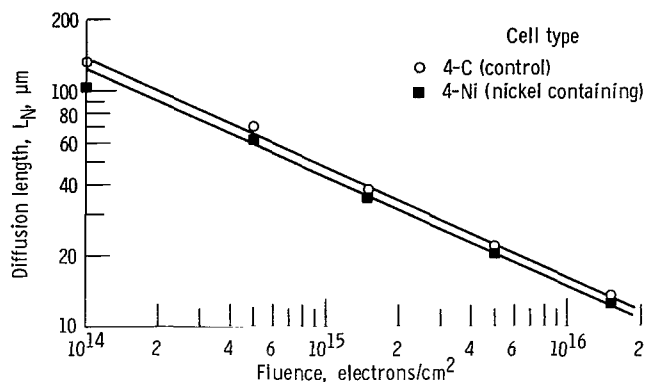


Figure 3. - Diffusion length as function of 1-MeV electron fluence.

the Ni cells is close to that of the controls. Therefore, the initial decrease in solar cell diffusion length due to Ni is not recovered during bombardment over the range of fluences studied.

Solar Simulator Data

The average spectral response with maximum and minimum values for three unbombarded 4-Ni and three 4-C cells is shown in figure 4. The response in terms of milliampere output for a 2-square-centimeter cell (ref. 8) is plotted against the wavelength of the light illuminating the cell. None of the cells had antireflection coatings. At all wavelengths, the average response of the Ni cells was below the control cell value. The spectral responses of eleven of the bombarded cells were measured. This group consisted of two 2-C, three 2-Ni, three 4-C, and three 4-Ni cells. The spectral responses were measured at five different fluences between 5×10^{14} and 1.5×10^{16} . The results for the 4-Ni and 4-C cells at 5×10^{14} and 1.5×10^{16} electrons per square centimeter fluence are shown in figures 5 and 6. The 4-Ni cell response was below the control cell response in each case. A plot of the data for the 2-Ni and 2-C cells shows a similar result. The response of the 4-Ni cell that contained 2.4×10^{14} atoms of Ni per cubic centimeter was lower than the response of the 2-Ni cell that contained 1×10^{14} atoms of Ni per cubic centimeter. At the three intermediate fluences not shown, the responses were between the extremes of figures 5 and 6. In all cases, both the red and the blue response of the Ni cells is below that of the control cells.

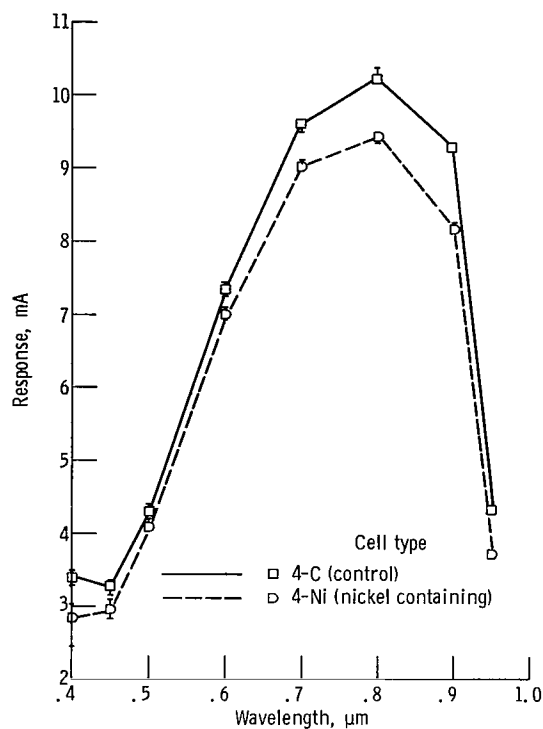


Figure 4. - Spectral response normalized for 2.0-square centimeter cells. Original un-bombarded values (three-cell average).

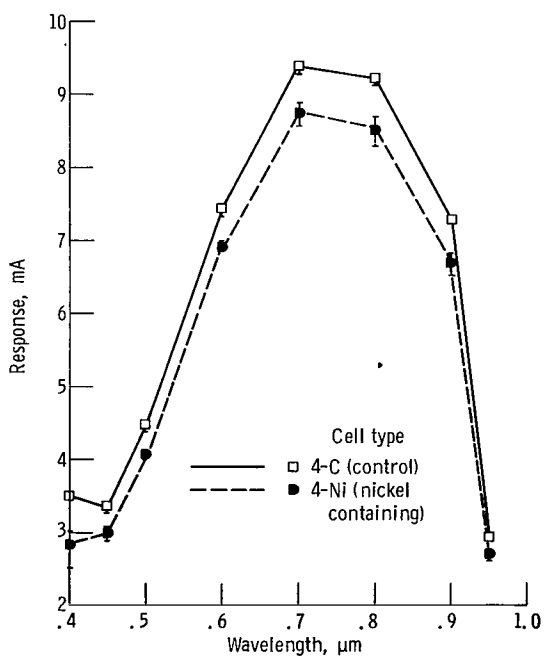


Figure 5. - Spectral response normalized for 2.0-square centimeter cells bombarded to fluence of 5×10^{14} electrons per square centimeter (three-cell average).

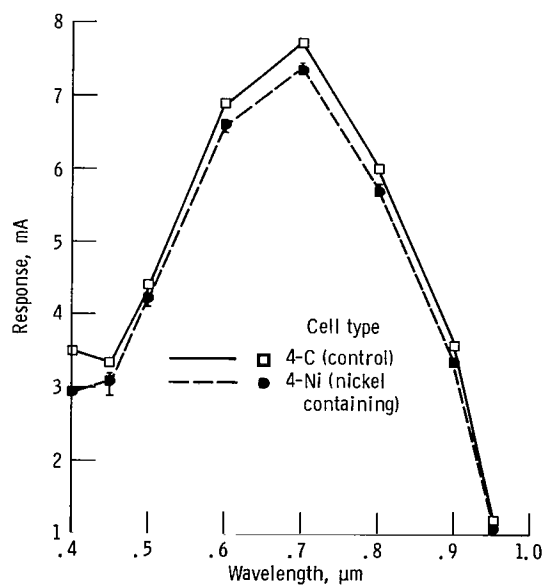


Figure 6. - Spectral response normalized for 2.0-square centimeter cells bombarded to fluence of 1.5×10^{16} electrons per square centimeter (three-cell average).

Other Data

Current-voltage data. - The unbombarded values of open-circuit voltage, short-circuit current, and fill factor of the Ni cells are shown in table IV to be below the control

TABLE IV. - INITIAL CELL PERFORMANCE

Cell type	Total number of cells	Average open-circuit voltage, V_{OC} , mV	Average short-circuit current, I_{SC} , mA	Average fill factor, percent
2-C (control cell)	6	548	61.1	74
2-Ni (nickel cell)	21	535	57.3	70
4-C (control cell)	3	542	61.1	72
4-Ni (nickel cell)	3	517	54.2	67

cell values. A plot of open-circuit voltage V_{OC} against fluence (fig. 7) for the 4-Ni and 4-C control cells shows that the values of V_{OC} of the 4-Ni cells are below the control cell V_{OC} values throughout the range of bombardment. A plot of short-circuit current

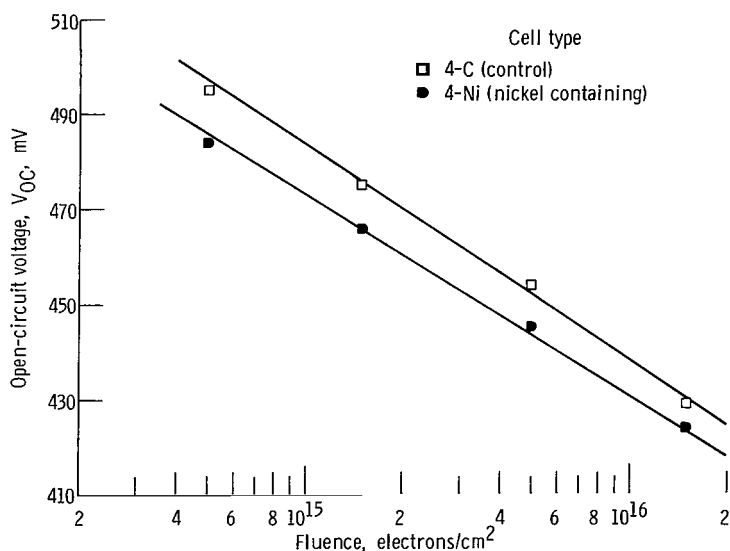


Figure 7. - Open-circuit voltage as function of 1-MeV electron fluence.

I_{SC} against fluence (fig. 8) similarly shows that the I_{SC} of the 4-Ni cells is below the I_{SC} of the 4-C control cells at all values of the bombardment fluence. The V_{OC} and I_{SC} of the 2-Ni cells are below the V_{OC} and I_{SC} of the 2-C control cells, but the amount of difference is not outside the range of experimental error.

Hall mobility data. - The majority carrier mobility μ_P was measured by the Hall method. Four diffused samples whose junctions had been removed by chemical etching

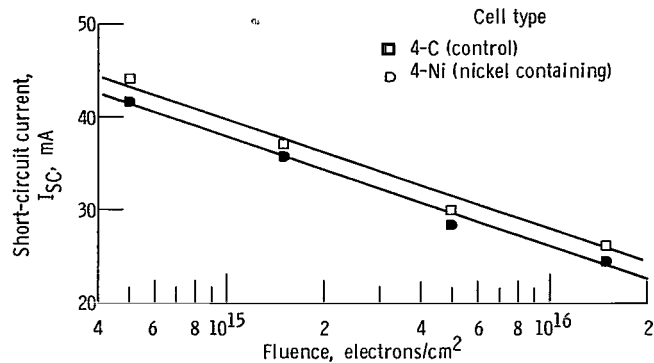


Figure 8. - Short-circuit current for 2.0-square centimeter cells as function of 1-MeV electron fluence.

and four undiffused samples were measured. The results are shown in table V. There is no significant difference in the majority carrier mobility of control and nickel or diffused and undiffused samples.

TABLE V. - MOBILITY DATA

Material	Sample	Mobility, (cm ²)(V ⁻¹)(sec ⁻¹)		Average minority carrier diffusion length, L _N , μm	Calculated minority carrier lifetime, τ _N , msec
		Majority, μ _P	Minority, μ _N		
4-C (control)	^a 27	373	1026	185	12.8
	28	369	1015	185	13.0
	52	372	1023	185	12.8
	^a 53	358	985	185	13.4
4-Ni (nickel)	^a 79	386	1061	125	5.6
	80	368	1012	125	5.8
	^a 93	358	985	125	6.0
2-Ni (nickel)	32	358	985	164	10.5

^aDiffused wafers with junctions removed.

The minority carrier mobility μ_N was calculated from the variation of the mobility ratio μ_P/μ_N with doping level (ref. 11). This value of μ_N and the average diffusion length of the sample type were used to calculate a minority carrier lifetime τ_N for the wafers by using the following relation:

$$L_n = \sqrt{\frac{kT}{q}} \mu_N \tau_N \quad (3)$$

where k is Boltzmann's constant, T is the temperature, and q is the electronic charge. The results are shown in table V. The samples of control material have lifetimes of 13.0 ± 0.1 microseconds. The 4-Ni samples have lifetimes of 5.8 ± 0.1 microseconds. The 2-Ni sample, which contained less Ni, had τ_N of 10.5 microseconds.

Infrared transmission measurements. - Optical absorption at a wavelength of 9 micrometers was used to detect oxygen in silicon with a room temperature sensitivity of 8×10^{16} oxygen atoms per cubic centimeter (ref. 12). To determine possible oxygen contamination, samples of Ni-doped and control silicon wafers with chemically polished surfaces were checked for oxygen content. The infrared transmission of an undiffused 4-Ni sample and diffused 4-C and 4-Ni samples was measured. The characteristic absorption peak at 9 micrometers was not observed for either type of material. Therefore, the oxygen content of both the Ni and the control material was less than 8×10^{16} atoms per cubic centimeter.

DISCUSSION

Nickel added to 10-ohm-centimeter boron-doped silicon degrades solar cell performance. This degradation was made apparent in two ways. First, the diffusion length was decreased. This decreased diffusion length was substantiated by the lower red response of the Ni-doped cell and was shown to be due to a decrease in carrier lifetime rather than to a change in the mobility. Second, the quality of the junction was degraded as shown by the lower open-circuit voltage and by a decrease in blue response of the cell. These effects are not caused by a concentration of oxygen above 8×10^{16} . The rate of diffusion-length degradation after 1-MeV electron bombardment is typical of 10-ohm-centimeter boron-doped cells. The Ni cells degrade as fast as the control cells and always have diffusion lengths lower than those of the control cells. Nickel precipitation in the bulk region of the Si cell may explain all of the observed effects. This explanation is supported by work done in the past on Ni in Si. Shattes and Wegener (ref. 13) used a plating and heating technique to prepare pulled silicon samples containing nickel. They inspected the samples with infrared light. Transmission photographs revealed patterns of lines and spots that they assumed were due to nickel precipitation at dislocations.

Similar work done by Tokumaru (ref. 14) showed that the number and patterns of the spots depended on the type of silicon used. Transmission photographs of float-zoned silicon with high dislocation density had many spots and a random pattern in which individual lines could not be distinguished. Low dislocation density pulled-crystal Si had fewer

spots forming distinct lines which presumably were dislocation lines.

Work done by Yoshida and Furusho (ref. 15) studied outdiffusion and precipitation of Ni in Si using radioactive ^{63}Ni . They concluded that nickel is dissolved interstitially to the solubility limit at the maximum temperature of the heating cycle and that interstitial Ni is not electrically active. During the cooling cycle, the Ni migrates to dislocations, precipitates, and distorts the silicon lattice. The precipitates are stable and, furthermore, act as nucleation centers for additional Ni precipitation during subsequent heat treatments.

In this present work, after the Ni was added by the starting-charge-only method, the wafers were subjected to an 840°C junction diffusion for 20 minutes. In addition, the application of electric contacts requires a heat treatment in the 550°C range for about 45 minutes. Although these heat treatments are at temperatures in the low range where the observations of precipitation by Yoshida and Furusho are more difficult to detect, it is likely that this precipitation is great enough to be observed as a decrease in solar cell performance.

When nickel precipitates in the junction region, the resulting strain may decrease the quality of the junction. This reduced junction quality would be observed as a loss of open-circuit voltage and a loss in the blue response of the cell. In addition, large amounts of Ni precipitation in the bulk region may cause recombination and decrease the diffusion length. The decreased diffusion length would be observed as a loss in the red response of the cell. All these losses were observed in the nickel-containing cells measured in this study.

A loss of red response in a cell could be caused by an impurity atom that reduces the lifetime. Iron and copper are both known to reduce the lifetime of minority carriers in p-type Si (ref. 16). However, the concentrations of iron and copper that could have been added to the silicon (from table I and eq. (2)) are at least four orders of magnitude lower than the Ni concentration. It is thus unlikely that they are responsible for the loss of red response noted in the cell. Additionally, an impurity that only reduces the lifetime would not produce the observed changes in open-circuit voltage or blue response. In view of these effects, it is likely that precipitation of Ni in the silicon lattice is responsible for the poor characteristics observed for the Ni-containing cells measured in this study.

CONCLUSIONS

A study was made of N on P solar cells made from boron-containing silicon (Si) that was doped with nickel. Measurements were made on these cells both before and after irradiation by 1-MeV electrons. The results of this study have lead to the following conclusions:

1. It is possible to add nickel (Ni) to Si by the starting-charge-only method with calculated Ni concentrations in the range of 10^{14} atoms per cubic centimeter.
2. Nickel lowers the initial unbombarded minority carrier diffusion length, the spectral response, the open-circuit voltage, and the short-circuit current of the cells.
3. The radiation resistance of the cells is not improved by addition of Ni. Performance of cells that contained Ni remains below that of undoped cells after irradiation with 1-MeV electrons to fluences of 1.5×10^{16} per square centimeter.
4. A possible cause of all the observed effects is Ni precipitation in the silicon crystal.

Lewis Research Center,
 National Aeronautics and Space Administration,
 Cleveland, Ohio, June 4, 1969,
 120-33-01-09-22.

REFERENCES

1. Mandelkorn, Joseph: New Silicon Solar Cell for Space Use. Proceedings of the 20th Annual Power Sources Conference. PSC Publications Committee, 1966, pp. 194-197.
2. Mandelkorn, Joseph: Improved Solar Cell. Proceedings of the 19th Annual Power Sources Conference. PSC Publications Committee, 1965, pp. 174-177.
3. Wysocki, J. J.; Rappaport, P.; Davison, E.; Hand, R.; and Loferski, J. J.: Lithium-Doped, Radiation-Resistant Silicon Solar Cells. Appl. Phys. Letters, vol. 9, no. 1, July 1, 1966, pp. 44-46.
4. Silverman, S. J.; and Singleton, J. B.: Technique for Preserving Lifetime in Diffused Silicon. J. Electrochem. Soc., vol. 105, no. 10, Oct. 1958, pp. 591-594.
5. Abdullaev, G. B.; Chelnokov, V. E.; Iskender-zade, Z. A.; and Dzhafarova, E. A.: The Effect of Transition Metal Impurities on the Lifetime Minority Carriers in N-Si. Radio Eng. Electr. Phys., vol. 11, June 1966, pp. 1012-1015.
6. Pfann, William G.: Zone Melting. Second ed., John Wiley & Sons, Inc., 1966.
7. Rosenzweig, W.: Diffusion Length Measurement by Means of Ionizing Radiation. Bell Syst. Tech. J., vol. 41, no. 5, Sept. 1962, pp. 1573-1588.
8. Mandelkorn, Joseph; Broder, Jacob D.; and Ulman, Robert P.: Filter-Wheel Solar Simulator. NASA TN D-2562, 1965.

9. Brandhorst, Henry W., Jr., and Hart, Russell E., Jr.: Radiation Damage to Cadmium Sulfide Solar Cells. NASA TN D-2932, 1965.
10. Mandelkorn, J.; McAfee, C.; Kesperis, J.; Schwartz, L.; and Pharo, W.: Fabrication and Characteristics of Phosphorous-Diffused Silicon Solar Cells. J. Electrochem. Soc., vol. 109, no. 4, Apr. 1962, pp. 313-318.
11. Phillips, Alvin B.: Transistor Engineering. McGraw-Hill Book Co., Inc., 1962, p. 69.
12. Kaiser, W.; Keck, P. H.; and Lange, C. F.: Infrared Absorption and Oxygen Content in Silicon and Germanium. Phys. Rev., vol. 101, no. 4, Feb. 15, 1956, pp. 1264-1268.
13. Shattes, Walter J.; and Wegener, H. A. R.: Lifetime and Nickel Precipitation in Silicon. J. Appl. Phys., vol. 29, no. 5, May 1958, p. 866.
14. Tokumaru, Yozo: Properties of Silicon Doped with Nickel. Jap. J. Appl. Phys., vol. 2, no. 9, Sept. 1963, pp. 542-547.
15. Yoshida, Masayuki; and Furusho, Katsuhisa: Behavior of Nickel as an Impurity in Silicon. Jap. J. Appl. Phys., vol. 3, no. 9, Sept. 1964, pp. 521-529.
16. Collins, C. B.; and Carlson, R. O.: Properties of Silicon Doped with Iron or Copper. Phys. Rev., vol. 108, no. 6, Dec. 15, 1957, pp. 1409-1414.

FIRST CLASS MAIL



POSTAGE AND FEES PAID
NATIONAL AERONAUTICS AND
SPACE ADMINISTRATION

POSTMASTER: If Undeliverable (Section 158
Postal Manual) Do Not Return

"The aeronautical and space activities of the United States shall be conducted so as to contribute . . . to the expansion of human knowledge of phenomena in the atmosphere and space. The Administration shall provide for the widest practicable and appropriate dissemination of information concerning its activities and the results thereof."

— NATIONAL AERONAUTICS AND SPACE ACT OF 1958

NASA SCIENTIFIC AND TECHNICAL PUBLICATIONS

TECHNICAL REPORTS: Scientific and technical information considered important, complete, and a lasting contribution to existing knowledge.

TECHNICAL NOTES: Information less broad in scope but nevertheless of importance as a contribution to existing knowledge.

TECHNICAL MEMORANDUMS: Information receiving limited distribution because of preliminary data, security classification, or other reasons.

CONTRACTOR REPORTS: Scientific and technical information generated under a NASA contract or grant and considered an important contribution to existing knowledge.

TECHNICAL TRANSLATIONS: Information published in a foreign language considered to merit NASA distribution in English.

SPECIAL PUBLICATIONS: Information derived from or of value to NASA activities. Publications include conference proceedings, monographs, data compilations, handbooks, sourcebooks, and special bibliographies.

TECHNOLOGY UTILIZATION PUBLICATIONS: Information on technology used by NASA that may be of particular interest in commercial and other non-aerospace applications. Publications include Tech Briefs, Technology Utilization Reports and Notes, and Technology Surveys.

Details on the availability of these publications may be obtained from:

**SCIENTIFIC AND TECHNICAL INFORMATION DIVISION
NATIONAL AERONAUTICS AND SPACE ADMINISTRATION
Washington, D.C. 20546**